

Symmetry and Topology in the Non-Hermitian Kitaev chain

Ayush Raj,^{1,*} Soham Ray,^{1,*} and Sai Satyam Samal^{1,*}

¹*Department of Physics and Astronomy, Purdue University, West Lafayette, Indiana 47907, USA*

We investigate the non-Hermitian Kitaev chain with non-reciprocal hopping amplitudes and asymmetric superconducting pairing. We work out the symmetry structure of the model and show that particle-hole symmetry (PHS) is preserved throughout the entire parameter regime. As a consequence of PHS, the topological phase transition point of a finite open chain coincides with that of the periodic (infinite) system. By explicitly constructing the zero-energy wave functions (Majorana modes), we show that Majorana modes necessarily occur as reciprocal localization pairs accumulating on opposite boundaries, whose combined probability density exhibits an exact cancellation of the non-Hermitian skin effect for the zero energy modes. Excited states, by contrast, generically display skin-effect localization, with particle and hole components accumulating at opposite ends of the system. At the level of bulk topology, we further construct a \mathbb{Z}_2 topological invariant in restricted parameter regimes that correctly distinguishes the topological and trivial phases. Finally, we present the topological phase diagram of the non-Hermitian Kitaev chain across a broad range of complex parameters and delineate the associated phase boundaries.

I. INTRODUCTION

Non-Hermitian quantum mechanics has engaged physicists for many years from various research areas, e.g. mathematical physics [1–5], complex space quantum mechanics [6, 7], and scattering theory [8]. More recently, researchers have been interested in understanding the quantum dynamics of open quantum systems, i.e. systems coupled with an environment [9–14] for their potential application in quantum optics [15, 16] and quantum information theory [17, 18]. Moreover, non-Hermitian generalizations of lattice models provide an excellent testbed to study phenomena ubiquitous to non-Hermitian physics, such as complex spectra, the appearance of exceptional points and the non-Hermitian skin effect (NHSE) i.e., exponential localization of the eigenstates towards one edge (or boundary) [19–32].

The Hatano-Nelson model [33], a generalization of tight-binding Hamiltonian with non-reciprocal hopping amplitude is an example of a system that exhibits NHSE. An unusual feature of such systems is the high sensitivity of the spectrum to the boundary conditions. This manifests itself in the fact that under periodic boundary conditions, the spectrum is complex and the system is unstable, but surprisingly in a finite open chain, the spectrum is purely real. The eigenstates, instead of being Bloch waves, localize exponentially toward one edge, giving rise to the NHSE.

In a set of seminal work [19, 34], it was shown that NHSE has a deep connection with topological properties of the system. It was shown that with non-reciprocal hoppings in the Su-Schrieffer-Heeger (SSH) model, the topological phase transition point in a finite open chain does not coincide with that of an infinite (or periodic) chain. The true transition point is governed by non-Bloch bulk-boundary correspondence, which is central to

topological non-Hermitian systems. This discovery has inspired a slew of research at the intersection of non-Hermitian physics and topology [14, 20–29, 31, 35–58].

This naturally raises the question of whether such behavior is universal in one-dimensional systems. By considering a non-Hermitian Kitaev chain [59–67] with non-reciprocal nearest neighbor hopping amplitudes (t_1 and t_2) and asymmetric superconducting pairing terms ($\Delta_1 e^{-i\varphi_1}$ and $\Delta_2 e^{i\varphi_2}$), see Fig. 1, we show that this is not generally the case. For a non-Hermitian Kitaev chain, cf. Fig. 1, the topological phase transition points for finite open chain coincides with that of an infinite (or periodic) chain. By performing a symmetry analysis, we show that particle-hole symmetry (PHS) always exists across the entire parameter regime and thereby protects the Majorana modes from NHSE. However, we show that particle and hole bulk modes exhibit an equal and opposite skin effect, which is also a consequence of PHS. Finally, we present the phase diagram for the non-Hermitian Kitaev chain in the complex chemical potential (μ) plane.

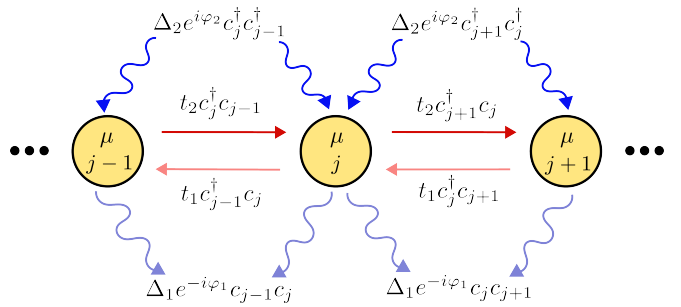


Figure 1. A caricature of the non-Hermitian Kitaev chain with non-reciprocal left and right hopping amplitudes, t_1 and t_2 and asymmetric superconducting pairing terms $\Delta_1 e^{-i\varphi_1}$ and $\Delta_2 e^{i\varphi_2}$. Each site is labeled by a positive integer j ($\in \mathbb{Z}^+$) and has a finite on-site (chemical) potential μ .

This article is organized as follows. In section II, we briefly review the topological phase transition in the Kitaev chain. In section III, we introduce non-reciprocal

* These authors contributed equally to this work.

hopping amplitudes and asymmetric superconducting pairing terms to construct a non-Hermitian Kitaev chain. Next, in section III A, we numerically obtain the band structure, ground state and first excited state for a finite chain, and compare with infinite chain. In section III B, we justify the robustness of Majorana zero modes to non-Hermiticity by considering the generalized Brillouin zone. In section III C, we study the symmetry structure of the non-Hermitian Kitaev chain in the complex parameter space. Finally, in section III D, we present topological phase diagrams with different parameter choices.

II. KITAEV CHAIN

The one-dimensional (1D) Kitaev chain exhibits topological phase transition with two distinct phases in the parameter space. It is a tight-binding chain with p -wave superconducting pairing terms and hosts Majorana edge states in the topological phase [59]. We begin with a brief review of the 1D (Hermitian) Kitaev chain [60] before investigating its non-Hermitian extension. The Hamiltonian with L lattice points, written in terms of particle creation (c_j^\dagger) and annihilation (c_j) operators on the j^{th} site is given as follows,

$$H = -\mu \sum_{j=1}^L c_j^\dagger c_j - \frac{1}{2} \sum_{j=1}^L \left(t c_j^\dagger c_{j+1} + \Delta e^{i\varphi} c_j c_{j+1} + h.c. \right), \quad (1)$$

where t is the hopping amplitude, Δ is the superconducting gap, φ is the superconducting phase and μ is the chemical potential. This system exhibits a topological phase transition [68] as we tune the parameters (t or μ) of the Hamiltonian. The topological phase is marked by the existence of Majorana zero edge modes in a finite chain [59, 60, 69].

In the case of an infinite ($L \rightarrow \infty$) chain, the energy spectrum can be obtained by performing a Fourier transform i.e., substituting $c_j = \frac{1}{\sqrt{L}} \sum_k e^{-ikj} d_k$ (for simplicity, the lattice constant is set to 1). The Hamiltonian in momentum space is of the form $H = \frac{1}{2} \sum_k \mathcal{D}_k^\dagger \mathcal{H}_k \mathcal{D}_k$, where,

$$\mathcal{H}_k = \begin{pmatrix} -t \cos k - \mu & i\Delta e^{-i\varphi} \sin k \\ -i\Delta e^{i\varphi} \sin k & t \cos k + \mu \end{pmatrix}, \quad (2)$$

and $\mathcal{D}_k^\dagger = (d_k^\dagger \ d_{-k})$. Diagonalizing \mathcal{H}_k one obtains the dispersion relation with gap-closing at $k = 0, \pm\pi$ and $|\mu| = t$, a necessary condition for topological phase transitions [60, 68].

In topological phase, ground state sub-space of the Kitaev chain, Eq. (1) is two-dimensional, corresponding to free dangling Majorana modes at two ends of the chain. The system remains in a topological phase whenever $|\mu| < t$ and in a trivial phase otherwise where there are no edge states. The distinction between trivial and topological phase can be compactly captured by defining

a \mathbb{Z}_2 -topological invariant. One writes the Hamiltonian, Eq. (2) in the form $\mathcal{H}_k = \vec{h}_k \cdot \vec{\sigma}$ and define \mathbb{Z}_2 -topological invariant as $\nu = \hat{h}_0 \cdot \hat{h}_\pi = \pm 1$ (where $\hat{h}_k = \frac{\vec{h}_k}{|\vec{h}_k|}$), with $+1$ corresponding to a trivial phase ($|\mu| > t$) and -1 to a topological phase ($|\mu| < t$).

III. NON-HERMITIAN KITAEV CHAIN

We now consider a non-Hermitian extension of the Kitaev chain, Eq. (1) and, modify the original Hamiltonian by introducing non-reciprocal hopping parameters and asymmetric superconducting pairing terms, as illustrated in Fig. 1. The Hamiltonian for the non-Hermitian Kitaev chain is given as follows,

$$H^{\text{NH}} = -\mu \sum_{j=1}^L c_j^\dagger c_j - \frac{1}{2} \sum_{j=1}^L (t_1 c_j^\dagger c_{j+1} + t_2 c_{j+1}^\dagger c_j) + \Delta_1 e^{-i\varphi_1} c_j c_{j+1} + \Delta_2 e^{i\varphi_2} c_{j+1}^\dagger c_j^\dagger, \quad (3)$$

where left hopping (t_1) and right hopping (t_2) amplitudes are different and also the superconducting pairing terms $\Delta_1 e^{-i\varphi_1}$ and $\Delta_2 e^{i\varphi_2}$ where $\Delta_1, \Delta_2 \in \mathbb{R}$.

For an infinite chain, we can perform a Fourier transform and obtain the Hamiltonian in the momentum space $H^{\text{NH}} = \frac{1}{2} \sum_k \mathcal{D}_k^\dagger \mathcal{H}_k^{\text{NH}} \mathcal{D}_k$, where,

$$\mathcal{H}_k^{\text{NH}} = \begin{pmatrix} -t_1 e^{-ik} - t_2 e^{ik} - 2\mu & 2i\Delta_2 e^{i\varphi_2} \sin k \\ -2i\Delta_1 e^{-i\varphi_1} \sin k & t_1 e^{ik} + t_2 e^{-ik} + 2\mu \end{pmatrix}, \quad (4)$$

and $\mathcal{D}_k^\dagger = (d_k^\dagger \ d_{-k})$. Diagonalizing the momentum space Hamiltonian Eq. (4), we obtain the two complex energy bands,

$$E_\pm(k) = i(t_2 - t_1) \sin k \pm \sqrt{4\Delta_1 \Delta_2 e^{i(\varphi_2 - \varphi_1)} \sin^2 k + [(t_1 + t_2) \cos k + 2\mu]^2}. \quad (5)$$

For simplicity, we assume that the parameters μ, t_1, t_2 are real and $\varphi_1 = \varphi_2 = 0$. In this case, we find that the spectrum, Eq. (5) is gapless whenever $k = 0, \pm\pi$ and $\mu = \pm\frac{1}{2}(t_1 + t_2)$. Hence, for an infinite chain, the gap closes at $|\mu| = \frac{1}{2}(t_1 + t_2)$, marking the topological phase transition for non-Hermitian Kitaev chain.

A. Finite non-Hermitian Kitaev chain

We now analyze the spectrum of a finite chain with open boundary conditions (OBC). The Hamiltonian of a finite chain with L lattice sites with OBC is represented

by a $2L \times 2L$ matrix as follows,

$$H^{\text{NH}} = \frac{1}{2} \Psi^\dagger \begin{pmatrix} A & B & 0 & 0 & 0 & \dots \\ C & A & B & 0 & 0 & \dots \\ 0 & C & A & B & 0 & \dots \\ 0 & 0 & C & A & B & \dots \\ \vdots & \vdots & \vdots & \vdots & \vdots & \ddots \end{pmatrix} \Psi, \quad (6)$$

where $\Psi^\dagger = (c_1^\dagger \ c_1 \ c_2^\dagger \ c_2 \ \dots)$ and A, B and C are 2×2 matrices,

$$\begin{aligned} A &= \begin{pmatrix} -\mu & 0 \\ 0 & \mu \end{pmatrix} & B &= \begin{pmatrix} -\frac{t_1}{2} & \frac{\Delta_2}{2} \\ -\frac{\Delta_1}{2} & \frac{t_2}{2} \end{pmatrix} \\ C &= \begin{pmatrix} -\frac{t_2}{2} & -\frac{\Delta_2}{2} \\ \frac{\Delta_1}{2} & \frac{t_1}{2} \end{pmatrix}, \end{aligned} \quad (7)$$

where we have again assumed for simplicity $\mu, t_1, t_2 \in \mathbb{R}$ and $\varphi_1 = \varphi_2 = 0$. Diagonalizing the Hamiltonian in Eq. (6) reveals a complex band structure, Fig. 2(b)-(c) and the presence of zero-energy modes in certain parameter regime, Fig. 2(a).

The band structure shows that the zero mode solutions only appear for certain values of the chemical potential μ , see Fig. 2(a), to be precise, the zero modes exist whenever we have $|\mu| < \frac{1}{2}(t_1 + t_2)$. This implies that the topological transition point derived using the spectrum of infinite chain, Eq. (5) coincides with the transition point obtained from the band structure of finite chain with OBC, cf. Fig. 2(a)-(b). In order to gain further insight, we look at the wave functions for the finite chain with OBC. With non-reciprocal hoppings ($t_1 \neq t_2$), one would naively expect to see the non-Hermitian skin effect (NHSE) [19]. However, we find that the zero modes do not show NHSE and remain robust to non-reciprocity, Fig. 3(a)-(c). The NHSE only appears when we consider wavefunctions corresponding to excited states, Fig. 3(d). In section III B and section III D, we present an explanation for the robustness of the zero modes to NHSE, Fig. 3(a)-(c), the presence of skin effect in excited states, Fig. 3(d).

B. Generalized Brillouin zone

The NHSE is an exponential localization of wave functions and is the result of a modified Brillouin zone (BZ) in non-Hermitian systems [19]. Simplest way to obtain the modified Brillouin zone is to make the substitution $e^{ika} \rightarrow \beta$ (note that a is the lattice constant and is set to one), where $|\beta|$ is determined by the non-reciprocity (or the non-Hermiticity) in the hopping parameters [19, 34]. Hamiltonian H^{NH} , Eq. (4) with the substitution $e^{ik} \rightarrow \beta$ becomes,

$$H^{\text{NH}}(\beta) = \begin{pmatrix} -t_1\beta^{-1} - t_2\beta - 2\mu & \Delta_2 e^{i\varphi_2}(\beta - \beta^{-1}) \\ \Delta_1 e^{-i\varphi_1}(\beta^{-1} - \beta) & t_1\beta + t_2\beta^{-1} + 2\mu \end{pmatrix}. \quad (8)$$

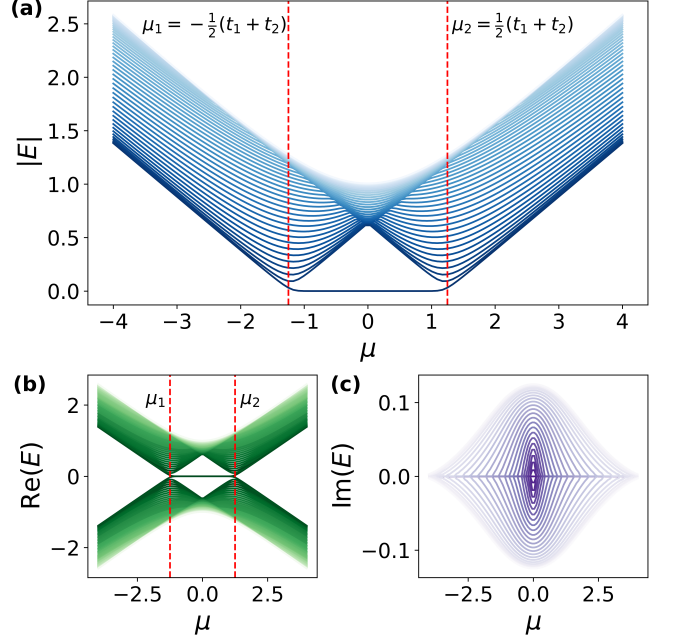


Figure 2. Energy bands of the finite ($L = 50$) non-Hermitian Kitaev chain with open boundary conditions (OBC) as function of the chemical potential, μ . Non-Hermiticity is introduced by choosing non-reciprocal hopping parameters i.e., left hopping parameter $t_1 = 1$ and right hopping parameter, $t_2 = 1.5$. The superconducting pairing terms are $\Delta_1 = 2 = \Delta_2$ and $\varphi_1 = 0 = \varphi_2$ cf. Eq. (3). (a) Absolute value of the energy bands as we vary the chemical potential μ . The zero modes (or the topological phase) appear whenever the chemical potential is fine tuned to lie between $\mu_1 = -\frac{1}{2}(t_1 + t_2)$ and $\mu_2 = \frac{1}{2}(t_1 + t_2)$. As a result of breaking Hermiticity, one obtains in general, a complex energy spectrum i.e. non-zero real part (b) and non-zero imaginary part (c) of the energy eigenvalues.

With the modified Hamiltonian, we can solve the eigenvalue equation, $\det(H^{\text{NH}}(\beta) - E) = 0$ to obtain the energy eigenvalues as a function of β . We are interested in understanding the behavior of the zero modes of the modified Hamiltonian, Eq. (8). For $E = 0$, we have, $\det H^{\text{NH}}(\beta) = 0$ and hence we have the following,

$$A_2[\beta^2 + \frac{1}{\beta^2}] + A_1[\beta + \frac{1}{\beta}] + A_0 = 0 \quad (9)$$

where

$$\begin{aligned} A_2 &= \Delta_1 \Delta_2 e^{i(\varphi_2 - \varphi_1)} - t_1 t_2 \\ A_1 &= -2\mu(t_1 + t_2) \\ A_0 &= -(t_1^2 + t_2^2 + 4\mu^2 + 2\Delta_1 \Delta_2 e^{i(\varphi_2 - \varphi_1)}). \end{aligned} \quad (10)$$

From Eq. (9) we find that if we have β_0 as a solution, then β_0^{-1} is also a solution. Hence, in general, we have four solutions to Eq. (9): $\beta_1, \beta_1^{-1}, \beta_2, \beta_2^{-1}$. Additionally, one can show that the matrix, Eq. (8) can be null only at the boundary of the topological and trivial phase, hence the rank of that matrix is 1 at all points in the topological

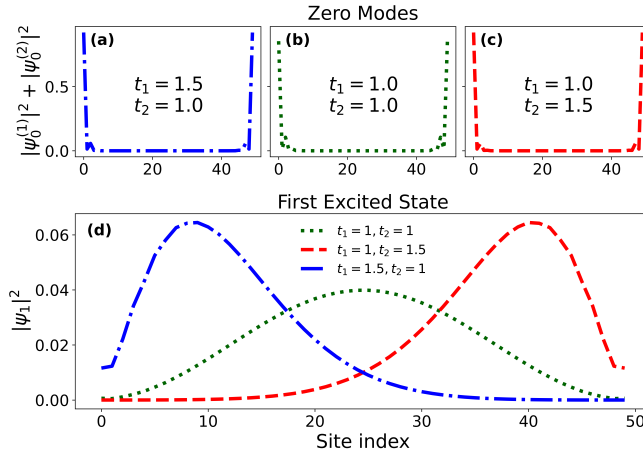


Figure 3. Probability density of the zero modes (doubly degenerate ground states) and first excited state in non-Hermitian Kitaev chain of length $L = 50$, with open boundary conditions (OBC) in the topological phase i.e., $|\mu| < \frac{1}{2}(t_1 + t_2)$. The chemical potential is $\mu = 0.2$ and the superconducting pairing terms are set to $\Delta_1 = 2 = \Delta_2$ with $\varphi_1 = 0 = \varphi_2$. The zero modes ($\psi_0^{(1)}$ and $\psi_0^{(2)}$) do not show any skin-effect with non-reciprocal hoppings. However, the first excited state (ψ_1) shows skin-effect (right or left localization) depending on the hopping parameters. (a) Sum of probability densities of zero mode wave functions, $\psi_0^{(1)}$ and $\psi_0^{(2)}$ with hopping parameters $t_1 = 1.5$ (left hopping), $t_2 = 1$ (right hopping). (b) Sum of probability densities of zero mode wave functions with reciprocal hoppings $t_1 = 1 = t_2$. (c) Sum of probability densities of zero mode wave functions with reversed reciprocities in hopping i.e., $t_1 = 1$ and $t_2 = 1.5$. (d) Probability density of the first excited state showing left localization (blue) with $t_1(= 1.5) > t_2(= 1)$, right localization (red) with $t_1(= 1) < t_2(= 1.5)$ in contrast to the case with reciprocal hoppings $t_1 = 1 = t_2$ (green).

phase. Hence, corresponding to each β , there is only one zero mode eigenvector in the topological phase. Thus, the four roots of Eq. (9) will have four zero mode eigenvectors in the topological phase. Specifically, at $\mu = 0$, we have $\beta_2 = -\beta_1$. On physical grounds, we expect that the zero mode eigenvectors corresponding to $\beta_1(\beta_1^{-1})$ will be the same as $-\beta_1(-\beta_1^{-1})$. Consequently, for $E = 0$, the two solutions have inverse localization factors β_1 and β_1^{-1} , which means that the solution β_1 (β_1^{-1}) localizes to the right (left) [62, 63, 65]. The total probability density of the zero-energy states is given by $|\psi_0^{(1)}|^2 + |\psi_0^{(2)}|^2$, where $\psi_0^{(1)}$ and $\psi_0^{(2)}$ are the normalized zero modes corresponding to factors β_1 and β_1^{-1} respectively. This reciprocal pairing eliminates the skin effect for zero-energy states.

The existence of the reciprocal solution pair can also be understood by the symmetries of the Kitaev chain. Particle-hole symmetry enforces solutions to be reciprocal pairs [62]. In section III C, we demonstrate that the particle-hole symmetry exists for arbitrary complex parameters in the Hamiltonian, thus protecting the Majorana edge modes, whenever they exist, for those param-

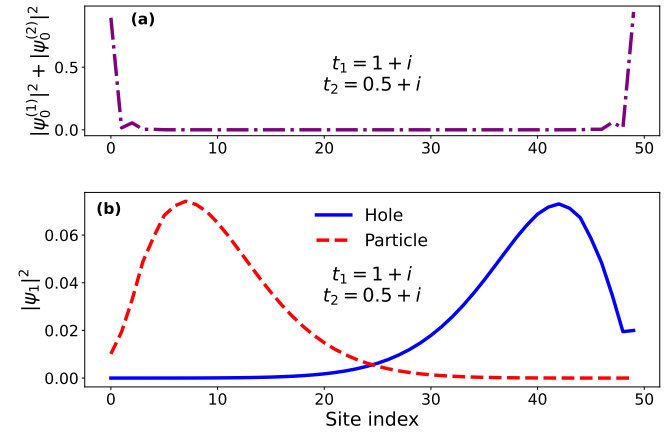


Figure 4. Probability density of zero mode wavefunctions and bulk mode wavefunctions of the non-Hermitian Kitaev chain with $L = 50$, $\mu = 0.2$, $t_1 = 1 + i$, $t_2 = 0.5 + i$, $\Delta_1 = 2 + i$ and $\Delta_2 = 1 + i$. The zero modes are immune to the NHSE whereas the particle and hole wavefunctions show an equal and opposite skin effect. (a) Sum of probability densities of the zero modes $\psi_0^{(1)}$ and $\psi_0^{(2)}$ is symmetric and localized at the edges. (b) The dashed red line denotes the probability density of the smallest positive energy (first excited state for a particle i.e., $+E > 0$) state and the solid blue line is the probability density of the smallest negative energy (first excited state for a hole i.e., $-E < 0$) state.

eter values. However, for any excited state (bulk mode), the solutions to $\det(H^{\text{NH}}(\beta) - E) = 0$ are not in a reciprocal pair. In fact, if β_1 is a solution corresponding to energy E , then β_1^{-1} is a solution corresponding to energy $-E$. Thus we expect an equal and opposite non-Hermitian skin effect for the particle and hole wavefunctions, cf. Fig. 4(b).

C. Symmetry analysis of non-Hermitian Kitaev chain

Our discussion so far has been focused on a simplified version of the non-Hermitian Kitaev chain, i.e., keeping the parameters t_1, t_2, μ real and setting $\varphi_1 = \varphi_2 = 0$. We now study the non-Hermitian Kitaev chain by relaxing this constraint. With complex parameters, the analysis done so far becomes cumbersome. However, understanding the symmetries of the system makes the analysis easier. Here, following Ref. [49], we study the symmetries of the non-Hermitian Kitaev chain.

In contrast to Hermitian systems, where the condition $H^\dagger = H$ (for Hamiltonian) ties together transpose and complex-conjugation operations, non-Hermitian Hamiltonians require that these operations be treated as independent when defining discrete symmetries. For example, when studying time-reversal symmetry (TRS) in a non-Hermitian system, one should address H^* and H^T separately, corresponding to TRS and its adjoint TRS^\dagger . Similar statements hold for chiral-symmetry (CS) and

particle-hole symmetry (PHS) [49]. Considering arbitrary complex parameters, cf. Eq. (3) and by using Specht's theorem [70], we find the symmetry classification for the non-Hermitian Kitaev chain as shown in Table I.

It is important to note that the particle-hole symmetry (PHS) always persists, with arbitrary complex parameters. The Table I presented here considers real μ . For complex μ , PHS still holds, and the only other possible symmetries are TRS † and CS † , see Appendix A. As a result of PHS, the Majorana zero modes exist and are robust across the entire parameter regime, Fig. 3(a)-(c) and Fig. 4(a). However, the bulk modes exhibit NHSE with particle and hole localizing at opposite edges, Fig. 4(b).

D. Topological phase diagram for non-Hermitian Kitaev chain

We have seen that the topological phase transition point coincides for a finite open chain and an infinite or periodic chain in the non-Hermitian Kitaev chain. Additionally, we found that the zero-mode solution exists for a range of values of the chemical potential μ , see Fig. 2. Hence, it is important to identify the topological and trivial phase in the non-Hermitian Kitaev chain, Eq. (3) as a function of the parameters. Therefore, we would like to have a topological invariant that can detect the phase, similar to the Hermitian version, cf. section II.

Similar to the Hermitian Kitaev chain [60], we begin by writing our Hamiltonian, Eq. (4) in the Pauli basis i.e., $H(k) = h_{\mathbb{I}}(k)\sigma_{\mathbb{I}} + h_x(k)\sigma_x + h_y(k)\sigma_y + h_z(k)\sigma_z$, where $\sigma_{\mathbb{I}}$ is the identity matrix and $\sigma_x, \sigma_y, \sigma_z$ are the Pauli matrices. The coefficients $h_{\mathbb{I}}(k), h_x(k), h_y(k)$ and $h_z(k)$

Condition	TRS	PHS	TRS †	PHS †	CS	CS †
$t_1 = t_2, \varphi_1 = \varphi_2$	✓	✓	✓	✓	✓	✓
$t_1 = t_2, \varphi_1 \neq \varphi_2$	✗	✓	✓	✗	✗	✓
$t_1 \neq t_2, \varphi_1 = \varphi_2$	✓	✓	✗	✗	✓	✗
$t_1 \neq t_2, \varphi_1 \neq \varphi_2$	✗	✓	✗	✗	✗	✗
$t_1 = t_2 \in \mathbb{C} \setminus \mathbb{R}, \varphi_1 = \varphi_2$	✗	✓	✓	✗	✗	✓
$t_1^* = t_2 \in \mathbb{C} \setminus \mathbb{R}, \varphi_1 = \varphi_2$	✗	✓	✗	✓	✗	✗
$t_1 \neq t_2 \in \mathbb{C} \setminus \mathbb{R}, \varphi_1 = \varphi_2$	✗	✓	✗	✗	✗	✗
$t_1 = t_2 \in \mathbb{C} \setminus \mathbb{R}, \varphi_1 \neq \varphi_2$	✗	✓	✓	✗	✗	✓
$t_1^* = t_2 \in \mathbb{C} \setminus \mathbb{R}, \varphi_1 \neq \varphi_2$	✗	✓	✗	✓	✗	✗
$t_1 \neq t_2 \in \mathbb{C} \setminus \mathbb{R}, \varphi_1 \neq \varphi_2$	✗	✓	✗	✗	✗	✗

Table I. Symmetries of the non-Hermitian Kitaev chain for general set of parameters. Hopping amplitudes t_1 and t_2 are chosen to be real ($t_1, t_2 \in \mathbb{R}$) unless specified otherwise. We also restrict ourselves to $\mu \in \mathbb{R}$ in this table. It is important to note that the superconducting pairing amplitudes Δ_1, Δ_2 do not affect the symmetries and therefore are unconstrained. Further, we also see that the particle hole symmetry is always present in the system and is the reason for the robustness of the Majorana zero-modes to the non-Hermitian skin effect.

are given as follows,

$$\begin{aligned} h_{\mathbb{I}}(k) &= i(t_1 - t_2) \sin k, \\ h_x(k) &= i(\Delta_2 e^{i\varphi_2} - \Delta_1 e^{-i\varphi_1}) \sin k, \\ h_y(k) &= -(\Delta_2 e^{i\varphi_2} + \Delta_1 e^{-i\varphi_1}) \sin k, \\ h_z(k) &= -(t_1 \cos k + t_2 \cos k + 2\mu). \end{aligned} \quad (11)$$

We begin with the simple case of real chemical potential ($\mu \in \mathbb{R}$), real hopping parameters ($t_1, t_2 \in \mathbb{R}$) and superconducting phases $\varphi_1 = \varphi_2 = 0$. We note that the gap in the bulk spectrum, Eq. (5) can only close at the points $k = 0, \pm\pi$, where we have $h_z(k=0) = -(t_1 + t_2 + 2\mu)$ and $h_z(k=\pm\pi) = (t_1 + t_2 - 2\mu)$. We can compactly define $\frac{[h_z(0)]}{|t_1 + t_2 + 2\mu|} = -\text{sgn}\{t_1 + t_2 + 2\mu\}$ and $\frac{[h_z(\pm\pi)]}{|t_1 + t_2 - 2\mu|} = \text{sgn}\{t_1 + t_2 - 2\mu\}$. This enables us to define the topological invariant in this simple case as follows,

$$\nu = \frac{[h_z(0)]}{|t_1 + t_2 + 2\mu|} \cdot \frac{[h_z(\pm\pi)]}{|t_1 + t_2 - 2\mu|}. \quad (12)$$

For $t_1 + t_2 \geq 2|\mu|$, we have $\nu = -1$, which is identified with the topological phase with two zero modes. In the case of $t_1 + t_2 < 2|\mu|$, we have $\nu = +1$, which corresponds to the trivial phase, cf. Fig. 2(a)-(c).

Next, we would like to understand the phase diagram with complex chemical potential ($\mu \in \mathbb{C}$) while keeping $t_1, t_2 \in \mathbb{R}$ and $\varphi_1 = \varphi_2 = 0$. This leads to infinite number of gap closing points in the complex μ -plane, Fig. 5 in contrast to only two solutions for real μ . The transition points along the $\text{Im}(\mu)$ axis can be obtained by noting that the gap closing points are at $k = \pm\pi/2$. This gives $\text{Im}(\mu) = \pm\sqrt{\Delta_1\Delta_2 + t_-^2}$, where $t_- = \frac{1}{2}(t_1 - t_2)$ and as shown in the Fig. 5(a). Similarly, the transition points along the $\text{Re}(\mu)$ axis are obtained by noting the gap closing points are at $k = 0, \pm\pi$ and gives the transition points at $\text{Im}(\mu) = \pm t_+$, where $t_+ = \frac{1}{2}(t_1 + t_2)$, Fig. 5(a). Additionally, with complex hopping amplitudes, it turns out that we can analytically determine four points on the phase boundary for a special case, where $\text{Im}(t_1) = \text{Im}(t_2)$. Gap-closing of the spectrum occurs at $k = 0, \pm\pi$ and $k = \pm\pi/2$ corresponding to the points $(0, \pm\sqrt{\Delta_1\Delta_2 + t_-^2})$ and $(\pm\text{Re}[t_+], \pm\text{Im}[t_+])$, cf. Fig. 5(b).

IV. CONCLUSION

The analysis presented here focuses on the non-Hermitian Kitaev chain where non-Hermiticity is introduced via non-reciprocal hopping amplitudes ($t_1 \neq t_2$) and asymmetric superconducting pairing terms ($\Delta_1 e^{-i\varphi_1} \neq \Delta_2 e^{i\varphi_2}$), cf. Eq. (3). Considering arbitrary complex parameters, we show the existence of different discrete symmetries corresponding to each parameter regime, see Table I.

We demonstrated that the transition point between the topological and trivial phase with periodic boundary

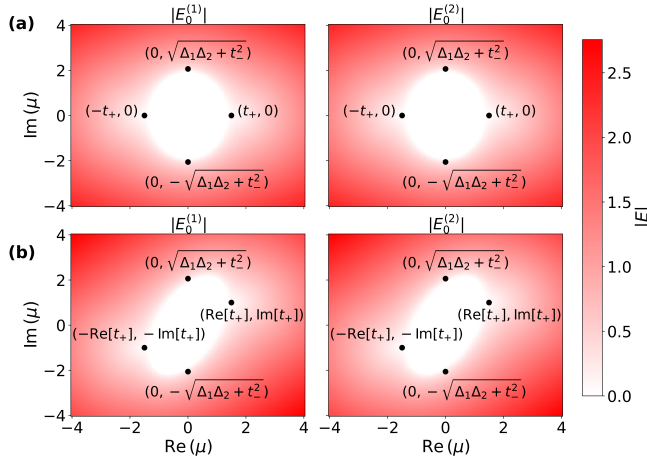


Figure 5. Topological phase diagram for non-Hermitian Kitaev chain in the complex chemical potential (μ) plane. The quantities $E_0^{(1)}$ and $E_0^{(2)}$ are the two lowest eigen-energies (absolute values) of the non-Hermitian Kitaev chain, Eq. (3). Vanishing of the two (eigen-energies, $E_0^{(1)}$ and $E_0^{(2)}$) corresponds to the Majorana-edge modes and hence marks the topological phase. (a) Phase diagram with non-reciprocal real hopping parameters. For obtaining the phase diagram we have used the following specific parameters, $t_1 = 1$, $t_2 = 2$, $\Delta_1 = 2$, $\Delta_2 = 2$, and $\varphi_1 = 0 = \varphi_2$. (b) Phase diagram with non-reciprocal complex hopping parameters with equal imaginary parts i.e., $\text{Im}(t_1) = \text{Im}(t_2)$. Specific choice of parameters for obtaining the phase diagram are as follows, $t_1 = 1 + i$, $t_2 = 2 + i$, $\Delta_1 = 2$, $\Delta_2 = 2$, and $\varphi_1 = 0 = \varphi_2$.

condition (equivalently infinite chain) coincides with the open boundary condition for a finite chain. The underlying reason is the existence of particle-hole symmetry across entire parameter regime, see Table I. As a result, the solutions to the localization parameter β , Eq. (9) for the zero modes (doubly degenerate) of the Hamiltonian always exist in reciprocal pairs [62, 63, 65] and therefore zero-modes are robust to non-Hermitian skin effect (NHSE), see Fig. 3(a)-(c) and Fig. 4(a). We also study the bulk (non-zero energy) modes and find that the particle and hole wavefunctions show equal and opposite skin

effect, as implied by PHS, see Fig. 4(b).

Further, we propose a topological invariant, Eq. (12) that determines the phase (trivial or topological) of a non-Hermitian Kitaev chain with real hopping amplitudes and chemical potential ($t_1, t_2, \mu \in \mathbb{R}$). Finally, by relaxing constraints on the parameters, we present phase diagrams for the non-Hermitian Kitaev chain in the complex chemical potential (μ) with real and imaginary hoppings, Fig. 5.

With recent experimental realization of non-Hermitian skin effect in mechanical metamaterials [71, 72], topoelectric circuits [73, 74] and photonic systems [40, 75–80], the interplay between topology and non-Hermiticity has become experimentally relevant. The versatility of these platforms allows for the engineering of a wide range of non-reciprocal couplings and effective interactions [81], making the realization of non-Hermitian Majorana physics a tangible prospect. In this work, we have provided a comprehensive characterization of the non-Hermitian Kitaev chain over the full complex parameter space, establishing a consistent correspondence between bulk topology, zero-energy Majorana modes, and phase boundaries. For specific parameter regimes, we obtained analytical expressions for points on the topological phase boundary, as illustrated in Fig. 5, offering concrete insight into the structure of the phase diagram. It remains to be seen whether the phase diagram can be determined analytically in full generality, including a characterization of the shape of the phase boundary; nevertheless, our results lay a systematic and broadly applicable foundation for exploring non-Hermitian topological phase transitions in this and related models.

Acknowledgements

We thank Jukka I. Vayrynen and Qi Zhou for insightful comments and discussions. A.R. would also like to thank Laimei Nie and Eric Schultz for useful discussions. We also thank Sayak Ray for comments on the draft of the manuscript.

Appendix A: Symmetry analysis for non-Hermitian Kitaev chain

We now explicitly work out the discrete symmetries of the non-Hermitian Kitaev chain in different parameter regimes. The Hamiltonian for a finite chain is given as follows,

$$H^{\text{NH}} = -\mu \sum_{j=1}^L c_j^\dagger c_j - \frac{1}{2} \sum_{j=1}^L (t_1 c_j^\dagger c_{j+1} + t_2 c_{j+1}^\dagger c_j + \Delta_1 e^{-i\varphi_1} c_j c_{j+1} + \Delta_2 e^{i\varphi_2} c_{j+1}^\dagger c_j), \quad (\text{A1})$$

In the case of an infinite ($L \rightarrow \infty$) chain, the energy spectrum can be obtained by performing a Fourier transform i.e., $c_j = \frac{1}{\sqrt{L}} \sum_k e^{-ikj} c_k$ (for simplicity, the lattice constant is set to 1), and obtain the Bogoliubov-de-Gennes (BdG)

Hamiltonian, $H_{\text{BdG}}^{\text{NH}} = \frac{1}{2} \sum_k \mathcal{C}_k^\dagger H(k) \mathcal{C}_k$, where,

$$H(k) = \begin{pmatrix} -t_1 e^{-ik} - t_2 e^{ik} - 2\mu & 2i\Delta_2 e^{i\varphi_2} \sin k \\ -2i\Delta_1 e^{-i\varphi_1} \sin k & t_1 e^{ik} + t_2 e^{-ik} + 2\mu \end{pmatrix} \quad (\text{A2})$$

and $\mathcal{C}_k^\dagger = (c_k^\dagger \ c_{-k})$. The discrete symmetries have been discussed in [49]. The spectral constraints arising from the possible symmetries of the system are summarized in the Table A1.

We now explore the possible symmetries of the non-Hermitian Kitaev chain and obtain Table I in the main text. The symmetries are unitary relations between 2×2 matrices, and a necessary and sufficient check is given by Specht's theorem, which states that two 2×2 matrices A and B are unitarily equivalent if and only if the following 3 criteria are satisfied

$$\text{Tr}[A] = \text{Tr}[B] \quad ; \quad \text{Tr}[A^2] = \text{Tr}[B^2] \quad ; \quad \text{Tr}[AA^\dagger] = \text{Tr}[BB^\dagger] \quad (\text{A3})$$

1. Time reversal symmetry (TRS)

For time reversal symmetry, we need to check if $H(-k)$ and $H(k)^*$ are unitarily related. The matrix forms are given as follows,

$$H(-k) = \begin{pmatrix} -t_1 e^{ik} - t_2 e^{-ik} - 2\mu & -2i\Delta_2 e^{i\varphi_2} \sin k \\ 2i\Delta_1 e^{-i\varphi_1} \sin k & t_1 e^{-ik} + t_2 e^{ik} + 2\mu \end{pmatrix} \quad (\text{A4})$$

$$H(k)^* = \begin{pmatrix} -t_1^* e^{ik} - t_2^* e^{-ik} - 2\mu^* & -2i\Delta_2 e^{-i\varphi_2} \sin k \\ 2i\Delta_1 e^{i\varphi_1} \sin k & t_1^* e^{-ik} + t_2^* e^{ik} + 2\mu^* \end{pmatrix} \quad (\text{A5})$$

and similarly, the Hermitian conjugates are,

$$H^\dagger(-k) = \begin{pmatrix} -t_1^* e^{-ik} - t_2^* e^{ik} - 2\mu^* & -2i\Delta_1 e^{i\varphi_1} \sin k \\ 2i\Delta_2 e^{-i\varphi_2} \sin k & t_1^* e^{ik} + t_2^* e^{-ik} + 2\mu^* \end{pmatrix} \quad (\text{A6})$$

$$H^\dagger(k)^* = \begin{pmatrix} -t_1 e^{-ik} - t_2 e^{ik} - 2\mu & -2i\Delta_1 e^{-i\varphi_1} \sin k \\ 2i\Delta_2 e^{i\varphi_2} \sin k & t_1 e^{ik} + t_2 e^{-ik} + 2\mu^* \end{pmatrix} \quad (\text{A7})$$

From here we evaluate the following,

$$\text{Tr}[H(-k)] = (t_2 - t_1)e^{ik} + (t_1 - t_2)e^{-ik} \quad (\text{A8})$$

$$\text{Tr}[H(k)^*] = (t_2^* - t_1^*)e^{ik} + (t_1^* - t_2^*)e^{-ik} \quad (\text{A9})$$

and similarly,

$$\begin{aligned} \text{Tr}[H(-k)^2] &= (t_1^2 + t_2^2)e^{i2k} + (t_1^2 + t_2^2)e^{-i2k} + 4\mu(t_1 + t_2)e^{ik} + 4\mu(t_1 + t_2)e^{-ik} + 8\mu^2 \\ &\quad + 4t_1 t_2 + 8\Delta_1 \Delta_2 e^{i\varphi_2 - i\varphi_1} \sin^2 k \end{aligned} \quad (\text{A10})$$

$$\begin{aligned} \text{Tr}[H(k)^{*2}] &= (t_1^{*2} + t_2^{*2})e^{-i2k} + (t_1^{*2} + t_2^{*2})e^{i2k} + 4\mu^*(t_1^* + t_2^*)e^{-ik} + 4\mu^*(t_1^* + t_2^*)e^{ik} + 8\mu^{*2} \\ &\quad + 4t_1^* t_2^* + 8\Delta_1 \Delta_2 e^{i\varphi_1 - i\varphi_2} \sin^2 k \end{aligned} \quad (\text{A11})$$

Table A1. Symmetries and their implications on the spectrum in momentum space

Symmetry	Eigenvalue pairs
TRS: $TH^*(k)T^{-1} = H(-k)$	$(E(k), E^*(-k))$
CS: $SH^\dagger(k)S^\dagger = -H(k)$	$(E(k), -E^*(k))$
PHS: $CH^T(k)C^{-1} = -H(-k)$	$(E(k), -E(-k))$
TRS [†] : $TH^T(k)T^{-1} = H(-k)$	$(E(k), E(-k))$
CS [†] (SLS): $\Gamma H(k)\Gamma^{-1} = -H(k)$	$(E(k), -E(k))$
PHS [†] : $CH^*(k)C^{-1} = -H(-k)$	$(E(k), -E^*(-k))$

Finally, we evaluate,

$$\begin{aligned} \text{Tr}[H(k)^* H^\dagger(k)^*] &= |t_1|^2 + t_1^* t_2 e^{i2k} + 2\mu t_1^* e^{ik} + t_1 t_2^* e^{-i2k} + |t_2|^2 + 2\mu t_2^* e^{-ik} + 2\mu^* t_1 e^{-ik} + 2\mu^* t_2 e^{ik} \\ &\quad + |t_1|^2 + t_1^* t_2 e^{-i2k} + 2\mu^* t_1^* e^{-ik} + t_1 t_2^* e^{i2k} + |t_2|^2 + 2\mu^* t_2^* e^{ik} + 2\mu^* t_1 e^{ik} + 2\mu^* t_2 e^{-ik} \\ &\quad + 4\Delta_2^2 \sin^2 k + 4\Delta_1^2 \sin^2 k + 8|\mu|^2 \end{aligned} \quad (\text{A12})$$

$$\begin{aligned} \text{Tr}[H(-k) H^\dagger(-k)] &= |t_1|^2 + t_1 t_2^* e^{i2k} + 2\mu^* t_1 e^{ik} + t_1^* t_2 e^{-2ik} + |t_2|^2 + 2\mu^* t_2 e^{-ik} + 2\mu t_1^* e^{-ik} + 2\mu t_2^* e^{ik} \\ &\quad + |t_1|^2 + t_1 t_2^* e^{-i2k} + 2\mu^* t_1 e^{-ik} + t_1^* t_2 e^{2ik} + |t_2|^2 + 2\mu^* t_2 e^{ik} + 2\mu t_1^* e^{ik} + 2\mu t_2^* e^{-ik} \\ &\quad + 4\Delta_1^2 \sin^2 k + 4\Delta_2^2 \sin^2 k + 8|\mu|^2 \end{aligned} \quad (\text{A13})$$

Hence, TRS exists if,

$$\begin{aligned} t_1, t_2 &\in \mathbb{R} \\ \varphi_1 &= \varphi_2 \\ \mu &\in \mathbb{R} \end{aligned} \quad (\text{A14})$$

2. Particle hole symmetry (PHS)

For particle hole symmetry (PHS), there must exist a unitary relation between $-H(-k)$ and $H(k)^T$. The full matrix forms are given as follows,

$$-H(-k) = \begin{pmatrix} t_1 e^{ik} + t_2 e^{-ik} + 2\mu & 2i\Delta_2 e^{i\varphi_2} \sin k \\ -2i\Delta_1 e^{-i\varphi_1} \sin k & -t_1 e^{-ik} - t_2 e^{ik} - 2\mu \end{pmatrix} \quad (\text{A15})$$

$$H(k)^T = \begin{pmatrix} -t_1 e^{-ik} - t_2 e^{ik} - 2\mu & -2i\Delta_1 e^{-i\varphi_1} \sin k \\ 2i\Delta_2 e^{i\varphi_2} \sin k & t_1 e^{ik} + t_2 e^{-ik} + 2\mu \end{pmatrix} \quad (\text{A16})$$

From here, we evaluate the Hermitian conjugates as follows,

$$-H^\dagger(-k) = \begin{pmatrix} t_1^* e^{-ik} + t_2^* e^{ik} + 2\mu^* & 2i\Delta_1 e^{i\varphi_1} \sin k \\ -2i\Delta_2 e^{-i\varphi_2} \sin k & -t_1^* e^{ik} - t_2^* e^{-ik} - 2\mu^* \end{pmatrix} \quad (\text{A17})$$

$$H^\dagger(k)^T = \begin{pmatrix} -t_1^* e^{ik} - t_2^* e^{-ik} - 2\mu^* & -2i\Delta_2 e^{-i\varphi_2} \sin k \\ 2i\Delta_1 e^{i\varphi_1} \sin k & t_1^* e^{-ik} + t_2^* e^{ik} + 2\mu^* \end{pmatrix} \quad (\text{A18})$$

Using this, we evaluate the following,

$$\text{Tr}[-H(-k)] = (t_1 - t_2)e^{ik} + (t_2 - t_1)e^{-ik} \quad (\text{A19})$$

$$\text{Tr}[H(k)^T] = (t_1 - t_2)e^{ik} + (t_2 - t_1)e^{-ik} \quad (\text{A20})$$

and

$$\begin{aligned} \text{Tr}[H(-k)^2] &= (t_1^2 + t_2^2)e^{i2k} + (t_1^2 + t_2^2)e^{-i2k} + 4\mu(t_1 + t_2)e^{ik} + 4\mu(t_1 + t_2)e^{-ik} \\ &\quad + 8\mu^2 + 4t_1 t_2 + 8\Delta_1 \Delta_2 e^{i\varphi_2 - i\varphi_1} \sin^2 k \end{aligned} \quad (\text{A21})$$

$$\begin{aligned} \text{Tr}[(H(k)^T)^2] &= (t_1^2 + t_2^2)e^{-i2k} + (t_1^2 + t_2^2)e^{i2k} + 4\mu(t_1 + t_2)e^{-ik} + 4\mu(t_1 + t_2)e^{ik} \\ &\quad + 8\mu^2 + 4t_1 t_2 + 8\Delta_1 \Delta_2 e^{i\varphi_2 - i\varphi_1} \sin^2 k \end{aligned} \quad (\text{A22})$$

Finally, we evaluate,

$$\begin{aligned} \text{Tr}[H(-k) H^\dagger(-k)] &= |t_1|^2 + t_1 t_2^* e^{2ik} + 2\mu^* t_1 e^{ik} + t_1^* t_2 e^{-2ik} + |t_2|^2 + 2\mu^* t_2 e^{-ik} + 2\mu t_1^* e^{-ik} + 2\mu t_2^* e^{ik} \\ &\quad + |t_1|^2 + t_1 t_2^* e^{-2ik} + 2\mu^* t_1 e^{-ik} + t_1^* t_2 e^{2ik} + |t_2|^2 + 2\mu^* t_2 e^{ik} + 2\mu t_1^* e^{ik} + 2\mu t_2^* e^{-ik} \\ &\quad + 4\Delta_1^2 \sin^2 k + 4\Delta_2^2 \sin^2 k + 8|\mu|^2 \end{aligned} \quad (\text{A23})$$

$$\begin{aligned} \text{Tr}[H(k)^T H^\dagger(k)^T] &= |t_1|^2 + t_1 t_2^* e^{-2ik} + 2\mu^* t_1 e^{-ik} + t_1^* t_2 e^{2ik} + |t_2|^2 + 2\mu^* t_2 e^{ik} + 2\mu t_1^* e^{ik} + 2\mu t_2^* e^{-ik} \\ &\quad + |t_1|^2 + t_1 t_2^* e^{2ik} + 2\mu^* t_1 e^{ik} + t_1^* t_2 e^{-2ik} + |t_2|^2 + 2\mu^* t_2 e^{-ik} + 2\mu t_1^* e^{-ik} + 2\mu t_2^* e^{ik} \\ &\quad + 4\Delta_1^2 \sin^2 k + 4\Delta_2^2 \sin^2 k + 8|\mu|^2 \end{aligned} \quad (\text{A24})$$

From here, we find that $-H(-k)$ and $H(k)^T$ are always unitarily related, i.e., PHS holds for all values of $t_1, t_2, \mu, \varphi_1, \varphi_2$.

3. Adjoint time reversal symmetry (TRS †)

For adjoint time reversal symmetry (TRS †), $H(-k)$ and $H(k)^T$ are unitarily related. The full matrix forms are,

$$H(-k) = \begin{pmatrix} -t_1 e^{ik} - t_2 e^{-ik} - 2\mu & -2i\Delta_2 e^{i\varphi_2} \sin k \\ 2i\Delta_1 e^{-i\varphi_1} \sin k & t_1 e^{-ik} + t_2 e^{ik} + 2\mu \end{pmatrix} \quad (\text{A25})$$

$$H(k)^T = \begin{pmatrix} -t_1 e^{-ik} - t_2 e^{ik} - 2\mu & -2i\Delta_1 e^{-i\varphi_1} \sin k \\ 2i\Delta_2 e^{i\varphi_2} \sin k & t_1 e^{ik} + t_2 e^{-ik} + 2\mu \end{pmatrix} \quad (\text{A26})$$

and the Hermitian conjugates are,

$$H^\dagger(-k) = \begin{pmatrix} -t_1^* e^{-ik} - t_2^* e^{ik} - 2\mu^* & -2i\Delta_1 e^{i\varphi_1} \sin k \\ 2i\Delta_2 e^{-i\varphi_2} \sin k & t_1^* e^{ik} + t_2^* e^{-ik} + 2\mu^* \end{pmatrix} \quad (\text{A27})$$

$$H^\dagger(k)^T = \begin{pmatrix} -t_1^* e^{ik} - t_2^* e^{-ik} - 2\mu^* & -2i\Delta_2 e^{-i\varphi_2} \sin k \\ 2i\Delta_1 e^{i\varphi_1} \sin k & t_1^* e^{-ik} + t_2^* e^{ik} + 2\mu^* \end{pmatrix} \quad (\text{A28})$$

Next, we evaluate the following,

$$\text{Tr}[H(-k)] = (t_2 - t_1)e^{ik} + (t_1 - t_2)e^{-ik} \quad (\text{A29})$$

$$\text{Tr}[H(k)^T] = (t_1 - t_2)e^{ik} + (t_2 - t_1)e^{-ik} \quad (\text{A30})$$

similarly,

$$\begin{aligned} \text{Tr}[H(-k)^2] &= (t_1^2 + t_2^2)e^{i2k} + (t_1^2 + t_2^2)e^{-i2k} + 4\mu(t_1 + t_2)e^{ik} + 4\mu(t_1 + t_2)e^{-ik} \\ &\quad + 8\mu^2 + 4t_1 t_2 + 8\Delta_1 \Delta_2 e^{i\varphi_2 - i\varphi_1} \sin^2 k \end{aligned} \quad (\text{A31})$$

$$\begin{aligned} \text{Tr}([H(k)^T]^2) &= (t_1^2 + t_2^2)e^{-i2k} + (t_1^2 + t_2^2)e^{i2k} + 4\mu(t_1 + t_2)e^{-ik} + 4\mu(t_1 + t_2)e^{ik} \\ &\quad + 8\mu^2 + 4t_1 t_2 + 8\Delta_1 \Delta_2 e^{i\varphi_2 - i\varphi_1} \sin^2 k \end{aligned} \quad (\text{A32})$$

Finally, we evaluate,

$$\begin{aligned} \text{Tr}[H(-k)H^\dagger(-k)] &= |t_1|^2 + t_1 t_2^* e^{i2k} + 2\mu^* t_1 e^{ik} + t_1^* t_2 e^{-i2k} + |t_2|^2 + 2\mu^* t_2 e^{-ik} + 2\mu t_1^* e^{-ik} + 2\mu t_2 e^{ik} \\ &\quad + |t_1|^2 + t_1 t_2^* e^{-i2k} + 2\mu^* t_1 e^{-ik} + t_1^* t_2 e^{i2k} + |t_2|^2 + 2\mu^* t_2 e^{ik} + 2\mu t_1^* e^{ik} + 2\mu t_2 e^{-ik} \\ &\quad + 4\Delta_1^2 \sin^2 k + 4\Delta_2^2 \sin^2 k + 8|\mu|^2 \end{aligned} \quad (\text{A33})$$

$$\begin{aligned} \text{Tr}[H(k)^T H^\dagger(k)^T] &= |t_1|^2 + t_1 t_2^* e^{-2ik} + 2\mu^* t_1 e^{-ik} + t_1^* t_2 e^{2ik} + |t_2|^2 + 2\mu^* t_2 e^{ik} + 2\mu t_1^* e^{ik} + 2\mu t_2^* e^{-ik} \\ &\quad + |t_1|^2 + t_1 t_2^* e^{2ik} + 2\mu^* t_1 e^{ik} + t_1^* t_2 e^{-2ik} + |t_2|^2 + 2\mu^* t_2 e^{-ik} + 2\mu t_1^* e^{-ik} + 2\mu t_2^* e^{ik} \\ &\quad + 4\Delta_1^2 \sin^2 k + 4\Delta_2^2 \sin^2 k + 8|\mu|^2 \end{aligned} \quad (\text{A34})$$

Hence, we find the following conditions for TRS † to hold,

$$\begin{aligned} \mu &\in \mathbb{C} \\ t_1 &= t_2 \in \mathbb{C} \\ \forall \varphi_1, \varphi_2 \end{aligned} \quad (\text{A35})$$

4. Adjoint particle hole symmetry (PHS †)

For adjoint particle hole symmetry (PHS †), there exists a unitary relation between $-H(-k)$ and $H(k)^*$. The matrix forms are,

$$-H(-k) = \begin{pmatrix} t_1 e^{ik} + t_2 e^{-ik} + 2\mu & 2i\Delta_2 e^{i\varphi_2} \sin k \\ -2i\Delta_1 e^{-i\varphi_1} \sin k & -t_1 e^{-ik} - t_2 e^{ik} - 2\mu \end{pmatrix} \quad (\text{A36})$$

$$H(k)^* = \begin{pmatrix} -t_1^* e^{ik} - t_2^* e^{-ik} - 2\mu^* & -2i\Delta_2 e^{-i\varphi_2} \sin k \\ 2i\Delta_1 e^{i\varphi_1} \sin k & t_1^* e^{-ik} + t_2^* e^{ik} + 2\mu^* \end{pmatrix} \quad (\text{A37})$$

From here, we obtain the Hermitian conjugates,

$$-H^\dagger(-k) = \begin{pmatrix} t_1^* e^{-ik} + t_2^* e^{ik} + 2\mu^* & 2i\Delta_1 e^{i\varphi_1} \sin k \\ -2i\Delta_2 e^{-i\varphi_2} \sin k & -t_1^* e^{ik} - t_2^* e^{-ik} - 2\mu^* \end{pmatrix} \quad (\text{A38})$$

$$H^\dagger(k)^* = \begin{pmatrix} -t_1 e^{-ik} - t_2 e^{ik} - 2\mu & -2i\Delta_1 e^{-i\varphi_1} \sin k \\ 2i\Delta_2 e^{i\varphi_2} \sin k & t_1 e^{ik} + t_2 e^{-ik} + 2\mu^* \end{pmatrix} \quad (\text{A39})$$

We now have,

$$\text{Tr}[-H(-k)] = (t_1 - t_2)e^{ik} + (t_2 - t_1)e^{-ik} \quad (\text{A40})$$

$$\text{Tr}[H(k)^*] = (t_2^* - t_1^*)e^{ik} + (t_1^* - t_2^*)e^{-ik} \quad (\text{A41})$$

Similarly, we obtain,

$$\begin{aligned} \text{Tr}[H(-k)^2] &= (t_1^2 + t_2^2)e^{i2k} + (t_1^2 + t_2^2)e^{-i2k} + 4\mu(t_1 + t_2)e^{ik} + 4\mu(t_1 + t_2)e^{-ik} + 8\mu^2 \\ &\quad + 4t_1 t_2 + 8\Delta_1 \Delta_2 e^{i\varphi_2 - i\varphi_1} \sin^2 k \end{aligned} \quad (\text{A42})$$

$$\begin{aligned} \text{Tr}[H(k)^{*2}] &= (t_1^{*2} + t_2^{*2})e^{-i2k} + (t_1^{*2} + t_2^{*2})e^{i2k} + 4\mu^*(t_1^* + t_2^*)e^{-ik} + 4\mu^*(t_1^* + t_2^*)e^{ik} + 8\mu^{*2} \\ &\quad + 4t_1^* t_2^* + 8\Delta_1 \Delta_2 e^{i\varphi_1 - i\varphi_2} \sin^2 k \end{aligned} \quad (\text{A43})$$

Finally, we have,

$$\begin{aligned} \text{Tr}[H(-k)H^\dagger(-k)] &= |t_1|^2 + t_1 t_2^* e^{2ik} + 2\mu^* t_1 e^{ik} + t_1^* t_2 e^{-2ik} + |t_2|^2 + 2\mu^* t_2 e^{-ik} + 2\mu t_1^* e^{-ik} + 2\mu t_2^* e^{ik} \\ &\quad + |t_1|^2 + t_1 t_2^* e^{-2ik} + 2\mu^* t_1 e^{-ik} + t_1^* t_2 e^{2ik} + |t_2|^2 + 2\mu^* t_2 e^{ik} + 2\mu t_1^* e^{ik} + 2\mu t_2^* e^{-ik} \\ &\quad + 4\Delta_1^2 \sin^2 k + 4\Delta_2^2 \sin^2 k + 8|\mu|^2 \end{aligned} \quad (\text{A44})$$

$$\begin{aligned} \text{Tr}[H(k)^* H^\dagger(k)^*] &= |t_1|^2 + t_1^* t_2 e^{i2k} + 2\mu t_1^* e^{ik} + t_1 t_2^* e^{-i2k} + |t_2|^2 + 2\mu t_2^* e^{-ik} + 2\mu^* t_1 e^{-ik} + 2\mu^* t_2 e^{ik} \\ &\quad + |t_1|^2 + t_1^* t_2 e^{-i2k} + 2\mu^* t_1^* e^{-ik} + t_1 t_2^* e^{i2k} + |t_2|^2 + 2\mu^* t_2^* e^{ik} + 2\mu^* t_1 e^{ik} + 2\mu^* t_2 e^{-ik} \\ &\quad + 4\Delta_2^2 \sin^2 k + 4\Delta_1^2 \sin^2 k + 8|\mu|^2 \end{aligned} \quad (\text{A45})$$

Hence, $-H(-k)$ and $H(k)^*$ are unitarily equivalent and PHS † holds if we have,

$$\begin{aligned} t_1 &= t_2^* \in \mathbb{C} \\ \mu &\in \mathbb{R} \\ \varphi_1 &= \varphi_2 \end{aligned} \quad (\text{A46})$$

5. Chiral symmetry (CS)

For the system to have chiral symmetry (CS), the Hamiltonians $-H(k)$ and $H(k)^\dagger$ must be unitarily related. The explicit matrix forms are given as follows,

$$-H(k) = \begin{pmatrix} t_1 e^{-ik} + t_2 e^{ik} + 2\mu & -2i\Delta_2 e^{i\varphi_2} \sin k \\ 2i\Delta_1 e^{-i\varphi_1} \sin k & -t_1 e^{ik} - t_2 e^{-ik} - 2\mu \end{pmatrix} \quad (\text{A47})$$

$$H(k)^\dagger = \begin{pmatrix} -t_1^* e^{ik} - t_2^* e^{-ik} - 2\mu^* & 2i\Delta_1 e^{i\varphi_1} \sin k \\ -2i\Delta_2 e^{-i\varphi_2} \sin k & t_1^* e^{-ik} + t_2^* e^{ik} + 2\mu^* \end{pmatrix} \quad (\text{A48})$$

The Hermitian conjugates are given as follows,

$$-H(k)^\dagger = \begin{pmatrix} t_1^* e^{ik} + t_2^* e^{-ik} + 2\mu^* & -2i\Delta_1 e^{i\varphi_1} \sin k \\ 2i\Delta_1 e^{-i\varphi_2} \sin k & -t_1^* e^{-ik} - t_2^* e^{ik} - 2\mu^* \end{pmatrix} \quad (\text{A49})$$

$$H(k) = \begin{pmatrix} -t_1 e^{-ik} - t_2 e^{ik} - 2\mu & 2i\Delta_2 e^{i\varphi_2} \sin k \\ -2i\Delta_1 e^{-i\varphi_1} \sin k & t_1 e^{ik} + t_2 e^{-ik} + 2\mu \end{pmatrix} \quad (\text{A50})$$

From here we obtain the following,

$$\text{Tr}[-H(k)] = (t_1 - t_2)e^{-ik} + (t_2 - t_1)e^{ik} \quad (\text{A51})$$

$$\text{Tr}[H(k)^\dagger] = (t_1^* - t_2^*)e^{-ik} + (t_2^* - t_1^*)e^{ik} \quad (\text{A52})$$

Similarly, we have,

$$\text{Tr}[H(k)^2] = (t_1^2 + t_2^2)e^{i2k} + (t_1^2 + t_2^2)e^{-i2k} + 4\mu(t_1 + t_2)e^{ik} + 4\mu(t_1 + t_2)e^{-ik} \quad (\text{A53})$$

$$+ 4\mu^2 + 4t_1t_2 + 8\Delta_1\Delta_2e^{i\varphi_2-i\varphi_1}\sin^2 k \quad (\text{A54})$$

$$\text{Tr}([H(k)^\dagger]^2) = (t_1^{*2} + t_2^{*2})e^{i2k} + (t_1^{*2} + t_2^{*2})e^{-i2k} + 4\mu(t_1^* + t_2^*)e^{ik} + 4\mu(t_1^* + t_2^*)e^{-ik} \quad (\text{A55})$$

$$+ 4\mu^2 + 4t_1^*t_2^* + 8\Delta_1\Delta_2e^{i\varphi_1-i\varphi_2}\sin^2 k \quad (\text{A56})$$

And finally,

$$\begin{aligned} \text{Tr}[H(k)H^\dagger(k)] &= |t_1|^2 + t_1t_2^*e^{-i2k} + 2\mu^*t_1e^{-ik} + t_1^*t_2e^{i2k} + |t_2|^2 + 2\mu^*t_2e^{ik} + 2\mu t_1^*e^{ik} + 2\mu t_2^*e^{-ik} \\ &+ |t_1|^2 + t_1t_2^*e^{i2k} + 2\mu^*t_1e^{ik} + t_1^*t_2e^{-i2k} + |t_2|^2 + 2\mu^*t_2e^{-ik} + 2\mu t_1^*e^{-ik} + 2\mu t_2^*e^{ik} \\ &+ 4\Delta_1^2\sin^2 k + 4\Delta_2^2\sin^2 k + 8|\mu|^2 \end{aligned} \quad (\text{A57})$$

$$\begin{aligned} \text{Tr}[H(k)^\dagger H(k)] &= |t_1|^2 + t_1^*t_2e^{i2k} + 2\mu t_1^*e^{ik} + t_1t_2^*e^{-i2k} + |t_2|^2 + 2\mu t_2^*e^{-ik} + 2\mu^*t_1e^{-ik} + 2\mu^*t_2e^{ik} \\ &+ |t_1|^2 + t_1^*t_2e^{-i2k} + 2\mu t_1^*e^{-ik} + t_1t_2^*e^{i2k} + |t_2|^2 + 2\mu t_2^*e^{ik} + 2\mu^*t_1e^{ik} + 2\mu^*t_2e^{-ik} \\ &+ 4\Delta_1^2\sin^2 k + 4\Delta_2^2\sin^2 k + 8|\mu|^2 \end{aligned} \quad (\text{A58})$$

Hence, unitary equivalence between $-H(k)$ and $H(k)^\dagger$ exists and CS holds if we have,

$$\begin{aligned} t_1, t_2, \mu &\in \mathbb{R} \\ \varphi_1 &= \varphi_2 \end{aligned} \quad (\text{A59})$$

6. Adjoint chiral symmetry (CS †)

For the system to have adjoint chiral symmetry (CS †), the Hamiltonians $-H(k)$ and $H(k)$ are unitarily related. The explicit matrix forms are given as follows,

$$-H(k) = \begin{pmatrix} t_1e^{-ik} + t_2e^{ik} + 2\mu & -2i\Delta_2e^{i\varphi_2}\sin k \\ 2i\Delta_1e^{-i\varphi_1}\sin k & -t_1e^{ik} - t_2e^{-ik} - 2\mu \end{pmatrix} \quad (\text{A60})$$

$$H(k) = \begin{pmatrix} -t_1e^{-ik} - t_2e^{ik} - 2\mu & 2i\Delta_2e^{i\varphi_2}\sin k \\ -2i\Delta_1e^{-i\varphi_1}\sin k & t_1e^{ik} + t_2e^{-ik} + 2\mu \end{pmatrix} \quad (\text{A61})$$

The Hermitian conjugates are given as follows,

$$-H(k)^\dagger = \begin{pmatrix} t_1^*e^{ik} + t_2^*e^{-ik} + 2\mu^* & -2i\Delta_1e^{i\varphi_1}\sin k \\ 2i\Delta_1e^{-i\varphi_2}\sin k & -t_1^*e^{-ik} - t_2^*e^{ik} - 2\mu^* \end{pmatrix} \quad (\text{A62})$$

$$H(k)^\dagger = \begin{pmatrix} -t_1^*e^{ik} - t_2^*e^{-ik} - 2\mu^* & 2i\Delta_1e^{i\varphi_1}\sin k \\ -2i\Delta_2e^{-i\varphi_2}\sin k & t_1^*e^{-ik} + t_2^*e^{ik} + 2\mu^* \end{pmatrix} \quad (\text{A63})$$

From here we obtain the following,

$$\text{Tr}[-H(k)] = (t_1 - t_2)e^{-ik} + (t_2 - t_1)e^{ik} \quad (\text{A64})$$

$$\text{Tr}[H(k)] = (t_2 - t_1)e^{-ik} + (t_1 - t_2)e^{ik} \quad (\text{A65})$$

Since our matrices are related by an overall sign, we have,

$$\text{Tr}[H(k)^2] = \text{Tr}[\{-H(k)\}^2] \quad (\text{A66})$$

$$\text{Tr}[H(k)H(k)^\dagger] = \text{Tr}[\{-H(k)\}\{-H^\dagger(k)\}] \quad (\text{A67})$$

Hence, we have CS † if,

$$\begin{aligned} t_1 &= t_2 \in \mathbb{C} \\ \forall \varphi_1, \varphi_2, \mu \end{aligned} \quad (\text{A68})$$

[1] C. M. Bender and S. Boettcher, Real spectra in non-hermitian hamiltonians having PT-symmetry, [Phys. Rev. Lett. 80, 5243 \(1998\)](#).

[Lett. 80, 5243 \(1998\)](#).

[2] C. M. Bender, Making sense of non-hermitian hamiltonians, *Reports on Progress in Physics* **70**, 947 (2007).

[3] C. M. Bender, S. Boettcher, and P. N. Meisinger, PT-symmetric quantum mechanics, *Journal of Mathematical Physics* **40**, 2201 (1999).

[4] C. M. Bender, D. C. Brody, and H. F. Jones, Complex extension of quantum mechanics, *Phys. Rev. Lett.* **89**, 270401 (2002).

[5] A. Mostafazadeh, Exact pt-symmetry is equivalent to hermiticity, *Journal of Physics A: Mathematical and General* **36**, 7081 (2003).

[6] C. M. Bender and A. Turbiner, Analytic continuation of eigenvalue problems, *Physics Letters A* **173**, 442 (1993).

[7] H. F. Jones and J. Mateo, Equivalent hermitian hamiltonian for the non-hermitian $-x^4$ potential, *Phys. Rev. D* **73**, 085002 (2006).

[8] N. Moiseyev, Quantum theory of resonances: calculating energies, widths and cross-sections by complex scaling, *Physics Reports* **302**, 212 (1998).

[9] M. Liertzer, L. Ge, A. Cerjan, A. D. Stone, H. E. Türeci, and S. Rotter, Pump-induced exceptional points in lasers, *Phys. Rev. Lett.* **108**, 173901 (2012).

[10] H. Eleuch and I. Rotter, Resonances in open quantum systems, *Phys. Rev. A* **95**, 022117 (2017).

[11] I. de Vega and D. Alonso, Dynamics of non-markovian open quantum systems, *Rev. Mod. Phys.* **89**, 015001 (2017).

[12] A. Gómez-León, T. Ramos, A. González-Tudela, and D. Porras, Bridging the gap between topological non-hermitian physics and open quantum systems, *Phys. Rev. A* **106**, L011501 (2022).

[13] I. Rotter, A non-hermitian hamilton operator and the physics of open quantum systems, *Journal of Physics A: Mathematical and Theoretical* **42**, 153001 (2009).

[14] Y. Michishita and R. Peters, Equivalence of effective non-hermitian hamiltonians in the context of open quantum systems and strongly correlated electron systems, *Phys. Rev. Lett.* **124**, 196401 (2020).

[15] P. Rice, *An Introduction to Quantum Optics (Second Edition)*, 2053–2563 (IOP Publishing, 2025).

[16] Quantum trajectories iv, in *An Open Systems Approach to Quantum Optics: Lectures Presented at the Université Libre de Bruxelles October 28 to November 4, 1991* (Springer Berlin Heidelberg, Berlin, Heidelberg, 1993) pp. 155–173.

[17] H.-P. Breuer, E.-M. Laine, J. Piilo, and B. Vacchini, Colloquium: Non-markovian dynamics in open quantum systems, *Rev. Mod. Phys.* **88**, 021002 (2016).

[18] R. J. Lewis-Swan, A. Safavi-Naini, A. M. Kaufman, and A. M. Rey, Dynamics of quantum information, *Nature Reviews Physics* **1**, 627 (2019).

[19] S. Yao and Z. Wang, Edge states and topological invariants of non-hermitian systems, *Phys. Rev. Lett.* **121**, 086803 (2018).

[20] F. Song, S. Yao, and Z. Wang, Non-hermitian skin effect and chiral damping in open quantum systems, *Phys. Rev. Lett.* **123**, 170401 (2019).

[21] C. H. Lee and R. Thomale, Anatomy of skin modes and topology in non-hermitian systems, *Phys. Rev. B* **99**, 201103 (2019).

[22] H. Jiang, L.-J. Lang, C. Yang, S.-L. Zhu, and S. Chen, Interplay of non-hermitian skin effects and anderson localization in nonreciprocal quasiperiodic lattices, *Phys. Rev. B* **100**, 054301 (2019).

[23] L. Li, C. H. Lee, and J. Gong, Topological switch for non-hermitian skin effect in cold-atom systems with loss, *Phys. Rev. Lett.* **124**, 250402 (2020).

[24] K. Zhang, Z. Yang, and C. Fang, Correspondence between winding numbers and skin modes in non-hermitian systems, *Phys. Rev. Lett.* **125**, 126402 (2020).

[25] N. Okuma, K. Kawabata, K. Shiozaki, and M. Sato, Topological origin of non-hermitian skin effects, *Phys. Rev. Lett.* **124**, 086801 (2020).

[26] Q. Liang, D. Xie, Z. Dong, H. Li, H. Li, B. Gadway, W. Yi, and B. Yan, Dynamic signatures of non-hermitian skin effect and topology in ultracold atoms, *Phys. Rev. Lett.* **129**, 070401 (2022).

[27] K. Zhang, Z. Yang, and C. Fang, Universal non-hermitian skin effect in two and higher dimensions, *Nature Communications* **13**, 10.1038/s41467-022-30161-6 (2022).

[28] K. Kawabata, T. Numasawa, and S. Ryu, Entanglement phase transition induced by the non-hermitian skin effect, *Phys. Rev. X* **13**, 021007 (2023).

[29] G.-G. Liu, S. Mandal, P. Zhou, X. Xi, R. Banerjee, Y.-H. Hu, M. Wei, M. Wang, Q. Wang, Z. Gao, H. Chen, Y. Yang, Y. Chong, and B. Zhang, Localization of chiral edge states by the non-hermitian skin effect, *Phys. Rev. Lett.* **132**, 113802 (2024).

[30] W. Xu and Q. Zhou, *Excitonic skin effect* (2025), arXiv:2508.20027 [cond-mat.quant-gas].

[31] M. Sanahal, S. Panda, and S. Nandy, Gauge field induced skin effect in spinful non-hermitian systems, *Phys. Rev. B* **112**, 125149 (2025).

[32] Y.-M. Hu, Z. Wang, B. Lian, and Z. Wang, Many-body non-hermitian skin effect with exact steady states in the dissipative quantum link model, *Phys. Rev. Lett.* **135**, 260401 (2025).

[33] N. Hatano and D. R. Nelson, Localization transitions in non-hermitian quantum mechanics, *Phys. Rev. Lett.* **77**, 570 (1996).

[34] F. Song, S. Yao, and Z. Wang, Non-hermitian topological invariants in real space, *Phys. Rev. Lett.* **123**, 246801 (2019).

[35] M. Ezawa, Braiding of majorana-like corner states in electric circuits and its non-hermitian generalization, *Phys. Rev. B* **100**, 045407 (2019).

[36] N. Okuma and M. Sato, Non-hermitian topological phenomena: A review, *Annual Review of Condensed Matter Physics* **14**, 83–107 (2023).

[37] E. J. Bergholtz, J. C. Budich, and F. K. Kunst, Exceptional topology of non-hermitian systems, *Rev. Mod. Phys.* **93**, 015005 (2021).

[38] F. K. Kunst, E. Edvardsson, J. C. Budich, and E. J. Bergholtz, Biorthogonal bulk-boundary correspondence in non-hermitian systems, *Phys. Rev. Lett.* **121**, 026808 (2018).

[39] K. Yokomizo and S. Murakami, Non-bloch band theory of non-hermitian systems, *Phys. Rev. Lett.* **123**, 066404 (2019).

[40] L. Xiao, T. Deng, K. Wang, G. Zhu, Z. Wang, W. Yi, and P. Xue, Non-hermitian bulk-boundary correspondence in quantum dynamics, *Nature Physics* **16**, 761 (2020).

[41] D. S. Borgnia, A. J. Kruchkov, and R.-J. Slager, Non-hermitian boundary modes and topology, *Phys. Rev. Lett.* **124**, 056802 (2020).

[42] Z. Yang, K. Zhang, C. Fang, and J. Hu, Non-hermitian bulk-boundary correspondence and auxiliary generalized brillouin zone theory, *Phys. Rev. Lett.* **125**, 226402

(2020).

[43] S. Longhi, Topological phase transition in non-hermitian quasicrystals, *Phys. Rev. Lett.* **122**, 237601 (2019).

[44] J. C. Budich and E. J. Bergholtz, Non-hermitian topological sensors, *Phys. Rev. Lett.* **125**, 180403 (2020).

[45] Q. Zhang, Y. Li, H. Sun, X. Liu, L. Zhao, X. Feng, X. Fan, and C. Qiu, Observation of acoustic non-hermitian bloch braids and associated topological phase transitions, *Phys. Rev. Lett.* **130**, 017201 (2023).

[46] S.-Z. Li, X.-J. Yu, and Z. Li, Emergent entanglement phase transitions in non-hermitian aubry-andré-harper chains, *Phys. Rev. B* **109**, 024306 (2024).

[47] L. Xiao, T. Deng, K. Wang, Z. Wang, W. Yi, and P. Xue, Observation of non-bloch parity-time symmetry and exceptional points, *Phys. Rev. Lett.* **126**, 230402 (2021).

[48] A. Ghatak and T. Das, New topological invariants in non-hermitian systems, *Journal of Physics: Condensed Matter* **31**, 263001 (2019).

[49] K. Kawabata, K. Shiozaki, and S. Ryu, Many-body topology of non-hermitian systems, *Physical Review B* **105**, 10.1103/physrevb.105.165137 (2022).

[50] K. Kawabata, N. Okuma, and M. Sato, Non-bloch band theory of non-hermitian hamiltonians in the symplectic class, *Phys. Rev. B* **101**, 195147 (2020).

[51] A. McDonald, T. Pereg-Barnea, and A. A. Clerk, Phase-dependent chiral transport and effective non-hermitian dynamics in a bosonic kitaev-majorana chain, *Phys. Rev. X* **8**, 041031 (2018).

[52] A. Altland and M. R. Zirnbauer, Nonstandard symmetry classes in mesoscopic normal-superconducting hybrid structures, *Phys. Rev. B* **55**, 1142 (1997).

[53] K. Kawabata, K. Shiozaki, M. Ueda, and M. Sato, Symmetry and topology in non-hermitian physics, *Phys. Rev. X* **9**, 041015 (2019).

[54] L.-M. Chen, Y. Zhou, S. A. Chen, and P. Ye, Quantum entanglement and non-hermiticity in free-fermion systems, *Chin. Phys. Lett.* **41**, 127302 (2024).

[55] P. Brighi and A. Nunnenkamp, Pairing-induced phase transition in the non-reciprocal kitaev chain (2025), arXiv:2510.24851 [quant-ph].

[56] E. Medina-Guerra, I. V. Gornyi, and Y. Gefen, Correlations and krylov spread for a non-hermitian hamiltonian: Ising chain with a complex-valued transverse magnetic field, *Phys. Rev. B* **111**, 174207 (2025).

[57] E. Medina-Guerra, I. V. Gornyi, and Y. Gefen, Phase transitions in a non-hermitian su-schrieffer-heeger model via krylov spread complexity, *Phys. Rev. B* **112**, 035427 (2025).

[58] L. Jezequel, L. Herviou, and J. Bardarson, When and why non-hermitian eigenvalues miss eigenstates in topological physics (2026), arXiv:2601.05234 [cond-mat.mes-hall].

[59] A. Y. Kitaev, Unpaired majorana fermions in quantum wires, *Physics-Uspekhi* **44**, 131–136 (2001).

[60] J. Alicea, New directions in the pursuit of majorana fermions in solid state systems, *Reports on Progress in Physics* **75**, 076501 (2012).

[61] Q.-B. Zeng, B. Zhu, S. Chen, L. You, and R. Lü, Non-hermitian kitaev chain with complex on-site potentials, *Phys. Rev. A* **94**, 022119 (2016).

[62] Y. Li, Y. Cao, Y. Chen, and X. Yang, Universal characteristics of one-dimensional non-hermitian superconductors, *Journal of Physics: Condensed Matter* **35**, 055401 (2022).

[63] Y. Yan, W.-X. Cui, S. Liu, J. Cao, S. Zhang, and H.-F. Wang, Topological phase in a nonreciprocal kitaev chain, *New Journal of Physics* **25**, 123023 (2023).

[64] S. Sayyad and J. L. Lado, Topological phase diagrams of exactly solvable non-hermitian interacting kitaev chains, *Phys. Rev. Res.* **5**, L022046 (2023).

[65] S. Shen, W. Zhang, L. Huang, H. Liu, and Z. Zhang, Topological phase transition of non-hermitian systems with particle-hole symmetry, *physica status solidi (b)* **260**, 2200448 (2023).

[66] J. Cayao and R. Aguado, Non-hermitian minimal kitaev chains, *Phys. Rev. B* **111**, 205432 (2025).

[67] E. Ardonne and V. Kurasov, On the non-hermitian kitaev chain, *Journal of Physics A: Mathematical and Theoretical* **58**, 205302 (2025).

[68] X.-G. Wen, *Quantum Field Theory of Many-Body Systems: From the Origin of Sound to an Origin of Light and Electrons* (Oxford University Press, 2007).

[69] M. Aghaee, A. Alcaraz Ramirez, Z. Alam, et al., Interferometric single-shot parity measurement in inas–al hybrid devices, *Nature* **638**, 651 (2025).

[70] R. A. Horn and C. R. Johnson, *Matrix Analysis* (Cambridge University Press, 1985).

[71] A. Ghatak, M. Brandenbourger, J. van Wezel, and C. Coulais, Observation of non-hermitian topology and its bulk–edge correspondence in an active mechanical metamaterial, *Proceedings of the National Academy of Sciences* **117**, 29561 (2020).

[72] W. Wang, M. Hu, X. Wang, G. Ma, and K. Ding, Experimental realization of geometry-dependent skin effect in a reciprocal two-dimensional lattice, *Phys. Rev. Lett.* **131**, 207201 (2023).

[73] D. Zou, T. Chen, W. He, J. Bao, C. H. Lee, H. Sun, and X. Zhang, Observation of hybrid higher-order skin-topological effect in non-Hermitian topoelectrical circuits, *Nature Communications* **12**, 7201 (2021).

[74] L. Du, Y. Liu, M. Shi, S. Wang, Y. He, X. Zhou, X. Yang, L. Tao, K. Song, Z. Li, and X. Zhao, Experimental observation of interconversion of non-hermitian skin effect and anderson localization in a nonreciprocal topological circuit based on aubry-andré model, *Phys. Rev. B* **112**, 115417 (2025).

[75] S. Weidemann, M. Kremer, T. Helbig, T. Hofmann, A. Stegmaier, M. Greiter, R. Thomale, and A. Szameit, Topological funneling of light, *Science* **368**, 311 (2020).

[76] X. Zhu, H. Wang, S. K. Gupta, H. Zhang, B. Xie, M. Lu, and Y. Chen, Photonic non-hermitian skin effect and non-bloch bulk-boundary correspondence, *Phys. Rev. Res.* **2**, 013280 (2020).

[77] L. Zhang, Y. Yang, Y. Ge, Y.-J. Guan, Q. Chen, Q. Yan, F. Chen, R. Xi, Y. Li, D. Jia, S.-Q. Yuan, H.-X. Sun, H. Chen, and B. Zhang, Acoustic non-Hermitian skin effect from twisted winding topology, *Nature Communications* **12**, 6297 (2021).

[78] H. Gao, H. Xue, Z. Gu, T. Liu, J. Zhu, and B. Zhang, Non-Hermitian route to higher-order topology in an acoustic crystal, *Nature Communications* **12**, 1888 (2021).

[79] Q. Zhou, J. Wu, Z. Pu, J. Lu, X. Huang, W. Deng, M. Ke, and Z. Liu, Observation of geometry-dependent skin effect in non-Hermitian phononic crystals with exceptional points, *Nature Communications* **14**, 4569 (2023).

[80] T. Wan, K. Zhang, J. Li, Z. Yang, and Z. Yang, Observation of the geometry-dependent skin effect and dynamical

degeneracy splitting, [Science Bulletin](#) **68**, 2330 (2023).

[81] Y. Zhang and Z. Wei, Non-hermitian skin effect in non-hermitian optical systems, [Laser & Photonics Reviews](#) **19**, 2400099 (2025).